Genetic Programming-Based Model for Estimating Maximum Pull Load of FRP-to-Concrete Bond Interfaces with GUI Implementation

Abstract

This study presents a novel, interpretable machine learning framework for predicting the maximum pull load of fiber-reinforced polymer (FRP) bonded to concrete substrates. A comprehensive test database comprising 983 datasets was gathered from relevant existing studies. The datasets include key input parameters such as concrete compressive strength, bond length, width of FRP sheet, width of concrete block, FRP thickness, and elastic modulus of FRP sheets, with the maximum pull load as the output parameter. Utilizing this curated database, a symbolic regression model based on Genetic Programming (GP) was developed to uncover the nonlinear relationships among critical variables including axial stiffness of FRP, bond length, and concrete compressive strength. The model's predictive performance was evaluated using standard regression metrics, achieving mean absolute error (MAE) and root mean square error (RMSE) values below 5 kN, mean absolute percentage error (MAPE) slightly above 10%, and coefficient of determination (R2) exceeding 0.90 on both training and testing datasets. These results confirm the model's accuracy and generalizability. Unlike black-box models, symbolic regression offers an explicit mathematical expression, ensuring transparency and interpretability for engineering applications. To facilitate practical deployment, a user-friendly graphical user interface (GUI) named MaxPLoad-FRP-Concrete-GPaided-PredictionModel was developed, enabling practitioners to input key design parameters and obtain immediate, interpretable predictions. This tool serves as a valuable decision-support system in structural design and quality control of FRP strengthened concrete structures.

Keywords: Concrete, Fiber-reinforced polymer, Gene expression programming, and Machine learning technique, Pull load.

Graphical abstract

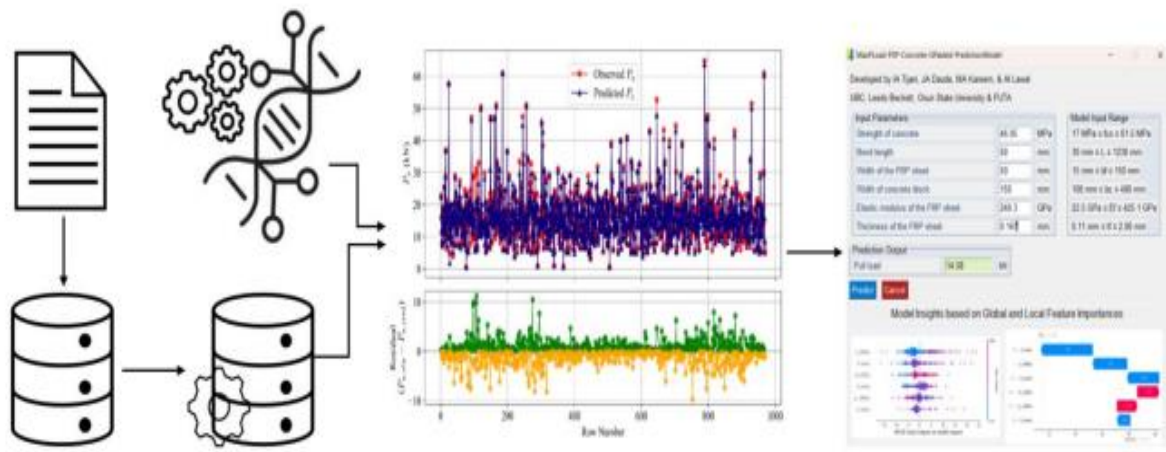

1. Introduction

Globally, some of the existing concrete structures have reached the end of their design service life. Besides, inappropriate maintenance, aging surface degradation, environmental action, and sudden increased service loads have caused concrete structures to weaken progressively. Hence, this led to a significant reduction in the load-carry capacity of the key structural components of infrastructures and subsequently resulted in safety issues. Accordingly, rehabilitation and retrofitting of the key structural components such as columnsbecome necessary. The application of fiber-reinforced polymer (FRP) has become a typical technology for strengthening and repairing aging and structurally deficient reinforced concrete structures [1–8]. The externally bonded reinforcement method is a common approach for applying FRP to strengthen and renovate structurally deficient reinforced concrete elements. Although FRP has many advantageous characteristics – such as high corrosion resistance, high durability under harsh environmental conditions, ease of handling, cost-effectiveness, and ease of transport, – there still exist some critical difficulties in the application of this technique. One of the most critical difficulties associated with externally bonded FRP technique is premature failure due to debonding. This may occur due to different debonding mechanisms between the FRP and concrete [9]. Generally, FRP debonding mechanisms are related to the damage process at the interface of bonded FRP to concrete, which typically affects the concrete region near the FRP layer. The damage process and propagation are triggered by the stress concentration presence between the FRP and concrete, and enhanced by the existence of concrete cracks. Also, the stiffness disparity of FRP and concrete, as well as localization mechanisms, significantly enhanced the FRP debonding mechanisms [10]. Generally, FRP debonding directly impacts the load-carrying capacity of the structure, with a subsequent outcome impairing the required ultimate capacity and desirable ductility of the structures. Typically, FRP debonding must be properly addressed for a safe structural design, to achieve the required nominal load-carrying capacity of the strengthened and rehabilitated structurally deficient reinforced concrete structures.

To further understand the debonding mechanisms, several experimental and theoretical studies have been conducted resulting in diverse analytical and empirical models to assess the bond-slip relationships [9,11–25]. Although different experimental setups have been adopted to examine the bond-slip relationship, most studies concluded that the concrete compressive strength, effective bond length, axial stiffness of FRP material, and width of concrete block, are the major factors affecting the bond mechanisms between the concrete and the FRP wraps. Nevertheless, despite the significant and numerous studies that have been undertaken on the bond-slip relationship of FRP sheet to concrete, the definition of a unified approach for a safe and satisfactory structural design associated with the debonding of FRP from strengthened and/or retrofitted concrete structures can still be considered as an open issue.

The existing developed models are based on the observations collected by various studies, hence making them more local to the experimental data. Also, most of the models are developed through conventional statistical analysis that might not consider high-level interaction or explicitly account for the randomness of the failure phenomenon [26]. Meanwhile, these limitations can be overcome through the use of machine learning techniques that are capable of solving a wide range of complex engineering problems [29–40]. The techniques can develop predictive models from datasets, without a need for comprehensive knowledge of the primary physical mechanisms. To the authors' best knowledge, there is a dearth of studies on the use of ML techniques to predict the bond strength of externally bonded FRP-to-concrete. Hence, this study aims to fill the knowledge and research gaps by using a gene expression model to develop a mathematical-based expression model for the prediction of the maximum pull load of externally bonded FRP-to-concrete interface.

2. Background of database development and machine learning

2.1 Overview of test database development

Several factors such as the compressive strength of concrete and axial stiffness of FRP materials have been identified to affect the bond strength of FRP-concrete, and yet the quantitative importance of such factors is unknown because debonding of FRP from strengthened concrete structures are typically regards as an open issue. For instance, an empirical model by Van Gemert [22] indicated that the width of FRP sheet, bond length, and tensile strength of concrete are the major factors affecting the bond strength, Yoshizawa and Wu [23] and Tanaka [41] stated that width of FRP sheet and the bond length are the main factors affecting the bond strength, while a group of authors [9,13,19,20] highlighted that axial stiffness of FRP, the width of FRP sheet, the width of concrete block, bond length, effective length, and compressive strength of concrete are the main factor affecting the bond strength of FRP-interface. Owing to the variations in the factors identified, analyzing the bond strength of FRP-to-concrete through ML techniques becomes attractive because these techniques are primarily established to handle variations in multiple parameters and solve complex real-world scenarios. As using these techniques to assess a phenomenon – in this study, pull load of FRP-concrete – requires the availability of a well-prepared database, thus a compressive review of the existing literature was carried out to locate bond strength test reports.

Typically, performing a bond-strength data-driven analysis is quite different from the conventional analysis approach. The bond strength of FRP-to-concrete can be evaluated through ML techniques that analyze bond-slip observations to arrive at an understanding of this phenomenon. The rationale behind adopting these techniques to examine the bond strength of FRP-concrete stems from the following hypothesis: (i) if bond-slip observations are collected from bond-slip tests, is it possible to apply ML technique to analyze the test observations to have a better understanding of bond strength of FRP-to-concrete, or (ii) at least to identify the key factors that influence the bond-slip relationship.

2.2 Machine learning

Machine learning (ML) is a computational method that receives and processes information to reach a suitable representation that best illustrates the circumstances embodied in the dataset. Typically, ML mimics a human-like reasoning process to solve complex problems that may not be properly explained using conventional methods or require advanced computing software [42]. Existing studies highlighted the successful application of contemporary ML techniques in civil engineering [43–46] and infrastructural management [47–49]. Typically, ML techniques provide four significant insights about a complex phenomenon (Fig. 1). These are i) descriptive insight – what happens between the data; ii) diagnostic insight – why did it happen; iii) predictive insight – what is likely to happen in the future because of the current observation; and iv) prescriptive insight – what is the best course of action. Irrespective of the type of insights to be provided, ML techniques often use evolutionary algorithms to learn the hidden pattern in the random points by conducting systematic analysis. Once a pattern is learned, the pattern becomes the benchmark in solving the scenario at hand via training and an adaptive learning process [42]. Hence, making the technique appropriate for a large dataset with a non-linear relationship between the variables and expected output, which is a typical relationship that occurs between the bond strength of FRP-concrete and input variables – axial stiffness of FRP, the width of FRP sheet, the width of concrete block, bond length, effective length, and compressive strength of concrete.

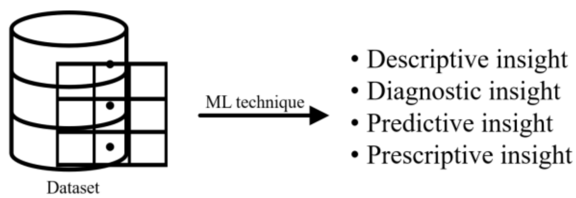

Fig. 1. Representation of insights provided by ML technique

Specifically, the ML technique in this study primarily uses gene expression programming (GEP), as a tool to derive a mathematical expression. GEP is a supervised ML technique mirroring biological evolution and human genetics based on the principles of Darwinian evolution for learning the hidden relations between several factors. This technique leverages genetic algorithms and genetic programming and advances their shortcomings [50,51] Usually, this ML technique performs symbolic regression using GEP operators to develop the mathematical function by programming chromosomes that are then conveyed as expression trees. By using bilingual and conclusive languages – known as Karva language – the genes in chromosomes are translated into head and tail accordingly. The genes are symbolized by functions, constants, and variables. The functions can be basic arithmetic, trigonometric, and/or any other mathematical operators (such as ^, exp, etc.). Meanwhile, the tail consists of numerical constants and/or variables – which are the input parameters of the scenario under consideration. The ML analysis is initialized with a random population of chromosomes and arrives at a solution. This solution is considered appropriate once a solution fulfills fitness criteria like correlation coefficients, mean absolute error, etc.

With the hope of bridging the knowledge and research gaps, this study presents a data-driven model that takes advantage of the ML learning technique to learn what happens between the dataset (i.e., descriptive analysis) to arrive at what is likely to happen based on the input information (i.e., predictive analysis) as well as prescriptive analysis – that is to determine which variable is the best course of action. This study develops a GEP-based mathematical expression suitable for independently evaluating and predicting the bond strength of FRP-to-concrete.

3. Research methodology

This section presents the proposed research procedure for building the dataset that will be used for a data-driven mathematical expression model for the bond strength of FRP-to-concrete. The research methodology consists of three main stages. Stage one – data aggregation – discusses the process of data collection from the existing related literature. The criteria for including test results were highlighted in this section. Subsequently, the aggregated data was analyzed in the second stage – data processing. Lastly, the third stage of the methodology is the development of a mathematical expression/model capable of uncovering the pattern hidden within the aggregated data for the prediction of the maximum pull load for the externally bonded FRP-to-concrete. Fig. (2) illustrates the general overview of the proposed research methodology adopted in this study.

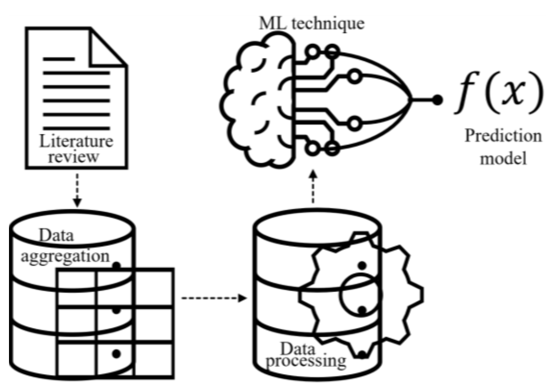

Fig. 2. Framework of the proposed methodology

3.1 Data aggregation and processing

The literature survey focuses on collecting test results on materials properties, sectional geometric, and compressive strength of concrete. The developed database compiled 990 data on bond-slip tests of FRP-concrete, all of which were conducted using different FRP materials and axial stiffness and spanned the period between 1999 and 2020. Due to variation in the researchers' backgrounds and norms of reporting test observations, some studies did not report certain information, and thus only 983 data points were appropriate for analysis. Inclusion of a test result into the database was based on the following criteria: (1) the FRP sheets were formed using the manual wet lay-up process; (2) No internal steel reinforcement was present (i.e., the specimen was made of plain concrete; and (3) the specimen was tested under pull-off tests, as illustrated in Fig. 3.

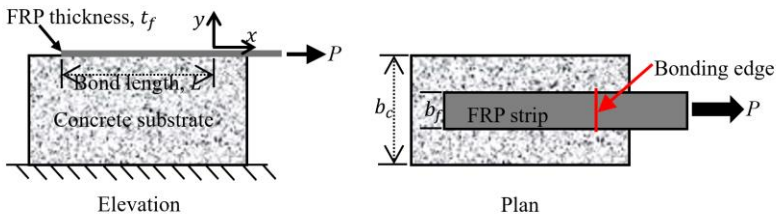

Fig. 3. Typical pull-off test setup

The collected data on the bond-slip tests covered 8 independent parameters: type of FRP sheets; strength of concrete f_{co}, bond length L, the width of the FRP sheet b_f, width of concrete block b_c, the elastic modulus of the FRP sheet E_f, the thickness of the FRP sheet t_f, and maximum pull load, P_u. For convenience, the outline of the complied database is provided in Table 1. This database is compiled from the existing studies [12,20,52–78]. Full details and more information can be found in their respective references.

Table 1. Outline of the database used in the model

Reference	Number of tests	Type of FRP sheets	f_{co} (MPa)	L (mm)	b_f (mm)	b_c (mm)	E_f (GPa)	t_f (mm)	P_u (kN)
Bizindavyi and Neale [62]	4	C, G	42.5	160–320	25.4	150	29.2–75.7	0.33–2.00	8.5–21.4
Nakaba et al. [72]	36	A, S, HS	23.8–57.8	300	50	100	124.1–425.1	0.165–0.193	9.35–25.63
Dai et al. [73]	26	A, C, G	33.1–35.0	210–330	100	150	74–230	0.11–0.381	15.6–64.8
Yao et al. [74]	72	C, G	18.9–27.1	75–240	15–100	100–150	22.5, 256	0.165, 1.27	3.81–19.07
Dai et al. [12]	26	A, C, G	35	330	100	400	74–230	0.11–1.14	13.5–60.9
Toutanji et al. [75]	12	C	17–61.5	100	50	200	110	0.495–0.99	7.56–19.03
Ko and Sato [76]	54	A, C, P	31.4	300	50	100	35–261	0.167–0.706	8.24–31.16
Hosseini and Mostofinejad [77]	9	C	44.2–46	100	48	150	238	0.131	9.32–11.83
Bilotta et al. [78]	18	C	21.46–26.00	50–400	50–100	150	230.0–241.0	0.166	16.85–24.96
Shi et al. [52]	27	B	44.6	200	50	100	81.5	0.156	15.01–20.9
Wu and Jiang [20]	65	C	25.3–59.02	30–400	50	150	238.1–248.3	0.167–0.501	7.38–30.15
Wu and Liu [53]	4	C	57.6	600	50	250	242	1.169	38.7–58.6
Zhou et al. [54]	12	C, G	56.1	300	50	100	79.96–243.74	0.167–0.17	13.44–18.32
Al-Allaf et al. [55]	55	C	40	100–200	50–150	200	240	0.118–0.236	0.47–29.69
Irshidat and Al-Saleh [56]	10	C, G	30	50–100	50–100	150	73–230	1	9.12–30
Shrestha et al. [57]	6	C	29.5	200	50	150	210–245	0.111–1.5	9.82–26.06
Mostofinejad et al. [58]	84	C	20–43	150	48	150	230–238	0.130–0.260	9.71–24.83
Sui et al. [59]	21	C	41.06	300	50	150	271.23	0.167	9.88–21.75
Wan et al. [60]	39	C	31.2–32.6	400	50	150	231	0.167	12.43–30.19
Yuan et al. [61]	12	B	39.87–44.24	200	50	150	73	0.12	8.27–11.44
Gao et al. [63]	7	H	59	730–1230	50	150–250	250	0.167	21–82
Moghaddas et al. [64]	94	C, G	22.68–48.28	200	30–60	150	76–230	0.11–0.34	3.90–20.76
Moghaddas and Mostofinejad [65]	136	C, G	22.70–48.20	200	30–60	150	76.0–230.0	0.11–0.34	4.76–25.49
Moshiri et al. [66]	10	C	38	240	50	150	165	1.4	25.29–77.73
Mostofinejad et al. [67]	52	C	23–35	200	50	150	230	0.166	10.2–14.98
Wei et al. [68]	12	B	30	210	100	100	84	0.167–0.501	17.6–25.4
Yuan et al. [69]	8	B	39.68	250	40	150	71–191	0.12–0.647	4.61–17.54
Li et al. [70]	62	C	24.32–48.48	200	35	100	251.49	0.167	6.63–24.32
Wang et al. [71]	10	C, B	30.5	150	50	100	91.0–231.0	0.111–0.167	13.76–36.63
Total	983		17.0–61.5	30–1230	15–150	100–400	22.5–425.1	0.11–2.00	0.47–230.4

Type of FRP sheets: A=Aramid, B=Basalt, C=Carbon, G=Glass, H=Hybrid, HS=High stiffness, and P=Polyacetal.

3.2 Normalization and evaluation metrics

The aggregated data in this study have different units of measurement that can lead to overfitting of a data-driven model. Existing studies stated that such datasets should be normalized to eliminate the effect of overfitting, [32,40]. Therefore, the aggregated data presented in Table 1 were normalized within the range of 0 and 1 using Eq. (1)

$$x_{nm} = \frac{(n_{\max} - n_{\min})(x - x_{\min})}{(x_{\max} - x_{\min})} + n_{\min} \tag{1}$$

where x_{nm} is the normalized model parameter, $x_{\min}$ and $x_{\max}$ are the minimum and maximum values of the actual model parameter x, $n_{\min}$ and $n_{\max}$ are the minimum and maximum values of the required normalization range.

To evaluate the performance of the proposed data-driven model, average value AV and integral absolute error IAE, as presented in Eqs. (2) and (3) were used as the error metrics and fitness indicators were adopted. The fitness indicators measure the degree of fitness of the predicted value to the aggregated data [6,79–81].

$$AV = \frac{\sum_1^n \frac{P_{v_i}}{A_{d_i}}}{N} \tag{2}$$

$$IAE = \frac{\sum_1^n \left| P_{v_i} - A_{d_i} \right|}{\sum_1^n \left| A_{d_i} \right|} \tag{3}$$

where P_{v_i} is the predicted values, A_{d_i} is the aggregated data and N is the number of datasets.

3.3 Development of data-driven model using gene expression programming

The proposed data-driven model learns the pattern hidden between six input variables - f_{co}, L, b_f, b_c, E_f, and t_f - and output variable P_u. The model development was performed in the GeneXproTools 5.0 software [82]. The variables were randomly gathered such that no specific aggregated data point was considered as a reference point. The data were separated into training and testing phases at the proportion of 70% and 30% of the aggregated dataset, respectively. Based on the existing studies and several test runs, the model fitting parameters were decided. The prediction model for the maximum pull load is encoded for solution and error metrics fitness functions are specified. The ML technique arbitrarily creates chromosomes and converts the chromosomes into expression trees. Thereafter, the error metrics fitness criteria for the solution are determined. If the error metrics fitness is sufficiently good, a solution is deemed appropriate. Hence, the analysis stops, and a typical prediction is obtained. Otherwise, the chromosomes are reproduced using roulette-wheel sampling and then converted to obtain a new generation [51,83,84]. Fig. (4) presents the closed-loop procedure for the development of the data-driven mathematical expression model.

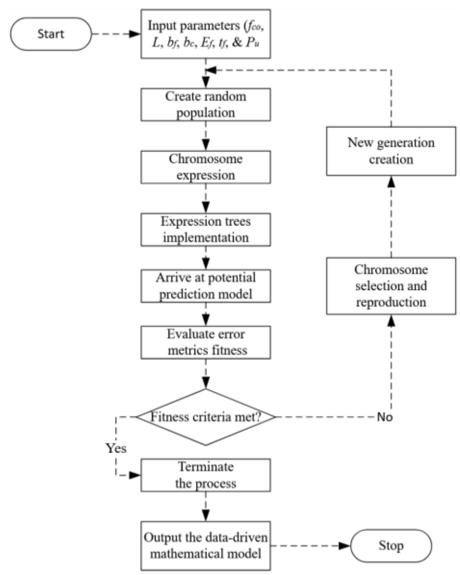

Fig. 4. Closed-loop procedure for the data-driven expression model

4. **Results and discussion**

4.1 Graphical illustration of the aggregated data

The distributions of the test database for the input parameters are shown in Fig. (5). The assembled database has 467 data points of bond length ranging from 100 – 200 mm, 211 and 170 data points of bond length ranging from 30 – 100 mm and 200 – 300 mm, respectively, while the remaining number of data points are distributed as shown in Fig. (3a). As shown in Fig. (3b), more data points – 397 – are concrete of 30 – 40 MPa strength followed by concrete strength of 20 – 30 MPa with 263 data points and 40 – 50 MPa concrete strength with 218 data points. Meanwhile, the database comprises many data points for the concrete block with a width of 100 – 150 mm and 244 data points for a concrete block with a width of less than 100 mm. A larger number of assembled observations falls within 25 – 50 mm FRP strip width, and the elastic modulus and thickness of the FRP have a substantial number of datasets within 200 – 250 GPa and 0.11 – 0.20 mm, respectively.

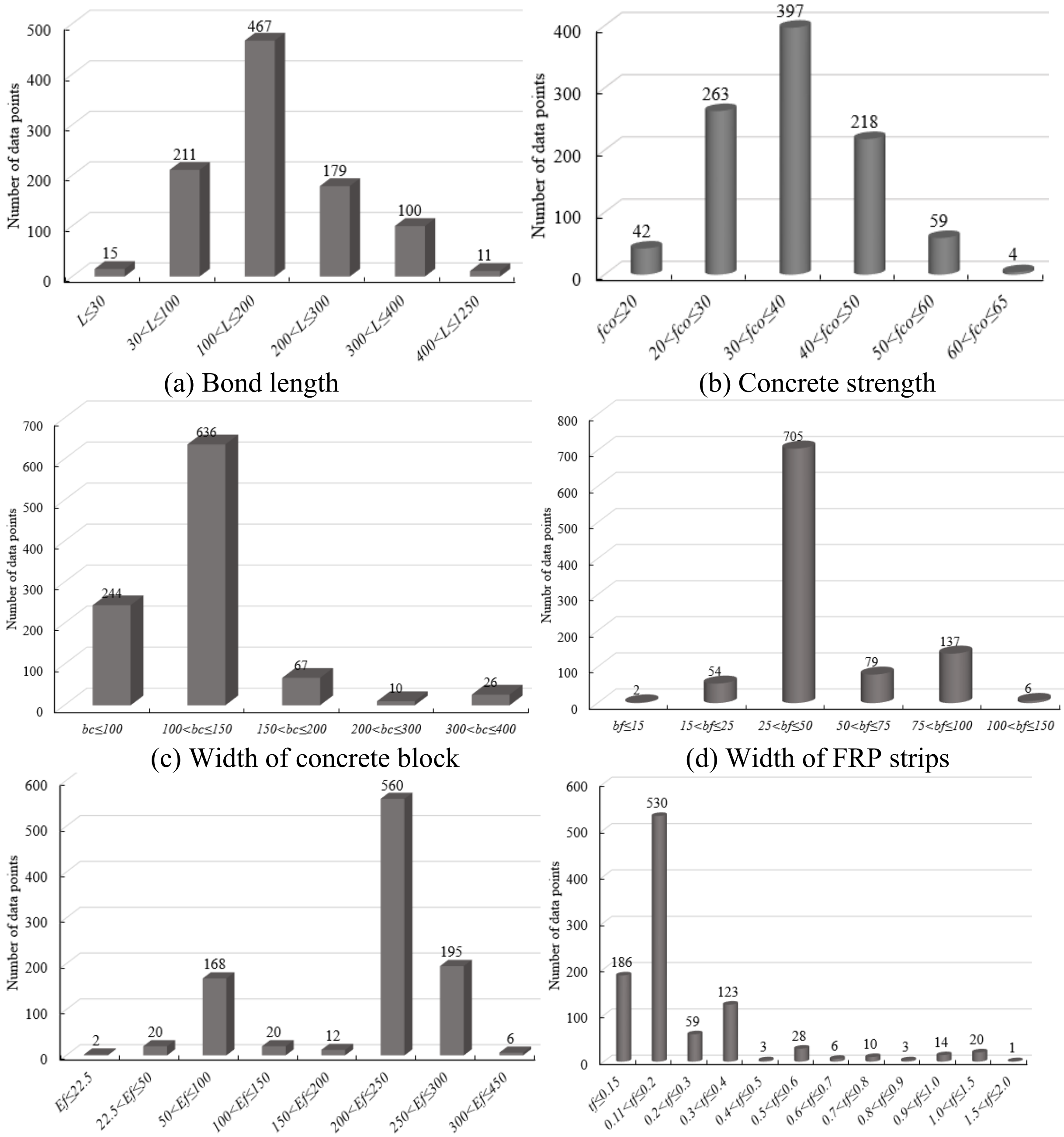

(a) Bond length (b) Concrete strength

(c) Width of concrete block (d) Width of FRP strips

(e) Elastic modulus of FRP sheets (f) Thickness of FRP strips

Fig. 5. Distribution of test database

4.2 Gene expression programming-based prediction model

Using the closed-loop procedure given in Fig. (4), the model was developed using the function fitness. Existing studies highlighted that an optimum solution is attained once the solution satisfies the fitness criteria governed by error metrics [51,83,84]. After running the model with the maximum error metrics fitness as the ending criteria, the obtained data-driven mathematical model is presented in Eq. (4).

$$P_u = y_1 + y_2 + y_3 + y_4 + y_5 + y_6 \tag{4}$$

$$y_1 = 0.05\left[\left(L - 118.34\right) + \left(L - 101.60\right)\right] t_f \tag{4a}$$

$$y_2 = \tan^{-1}\left[\left(1 - L - \sqrt[3]{f_{co}}\right) + \left(f_{co} + t_f E_f\right)\right] \tag{4b}$$

$$y_3 = \sqrt[3]{\tan\left(9.68L\right)} + \sqrt[3]{E_f - b_f - t_f b_f} \tag{4c}$$

$$y_4 = -1.13 b_f b_c \left[L t_f \left(\frac{E_f + b_f + f_{co}}{3} \right) \right]^{-1} \tag{4d}$$

$$y_5 = \left[\tan\left(GOE2A(b_c, L)\right)\right]^{-1} + avg\left(0.15, b_f\right) + \tan\left(b_c\right) \tag{4e}$$

$$y_6 = \exp\left[\ln \frac{b_f}{avg\left(L, b_f, -40.23\right)} + \tan^{-1}\left(L - b_f\right) \right] \tag{4f}$$

where GOE2A: if $x \geq y$, then x, else y.

By using the mathematical-based expression in Eq. (4), the predicted results are presented in Figs. (5) and (6). As illustrated in Fig. (5a), the predicted values and aggregated data were plotted on the y-axis and x-axis, respectively. The slope of the regression lines was observed as 92% and 94% for testing and training data respectively, which indicates a strong correlation between the aggregated data and predicted values by the mathematical-based expression model [85]. The correlation coefficient between the predicted values and aggregated data is 94.3%. Similarly, as presented in Fig. (5b), the average value for the model is approximately 1.0 and the integral absolute error of 0.09 is small, , suggesting that model's predictions are closer to the actual data. Existing studies highlighted that the closer the average value to 100% and the smaller the integral absolute error, the more accurate the model is indicating a the better overall result[79,86,87]. Hence, the developed mathematical-based expression model can predict the maximum pull load of externally bonded FRP-to-concrete.

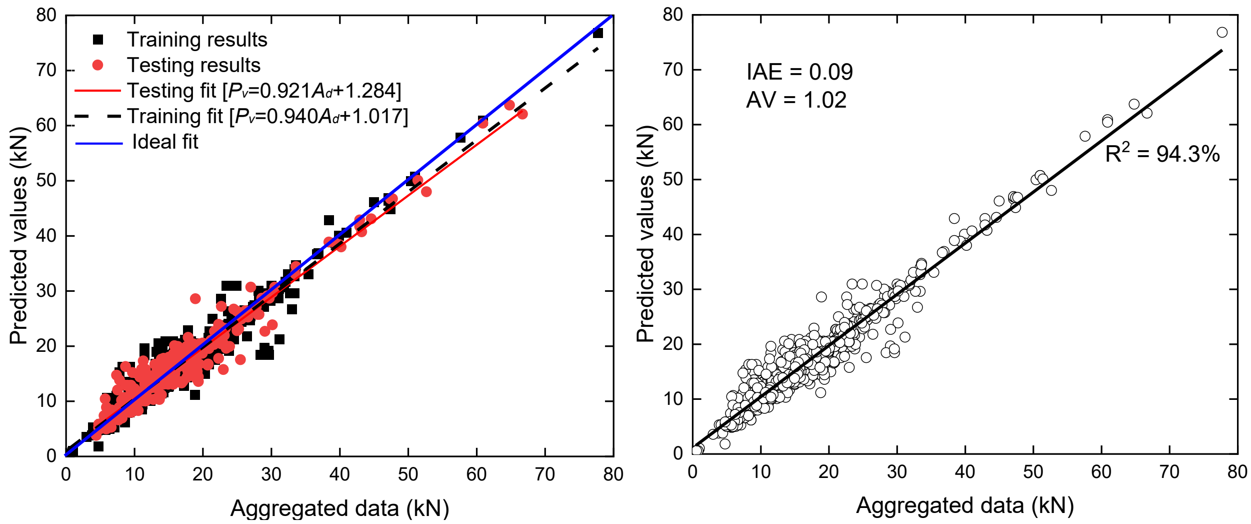

(a) Regression plot (b) fitness indicators

Fig. 6. Results comparison

The matching between the results generated based on the mathematical-based expression model and aggregated data is illustrated in Fig. (7a). The developed model's reliability was unquestionably shown by a small difference between the model-predicted and aggregated values. A similar observation could be seen when the predicted results and aggregated data were plotted against the axial stiffness of FRP materials (Fig 7b). Thereby, it can be inferred that the GEP-based mathematical expression model is appropriate and good.

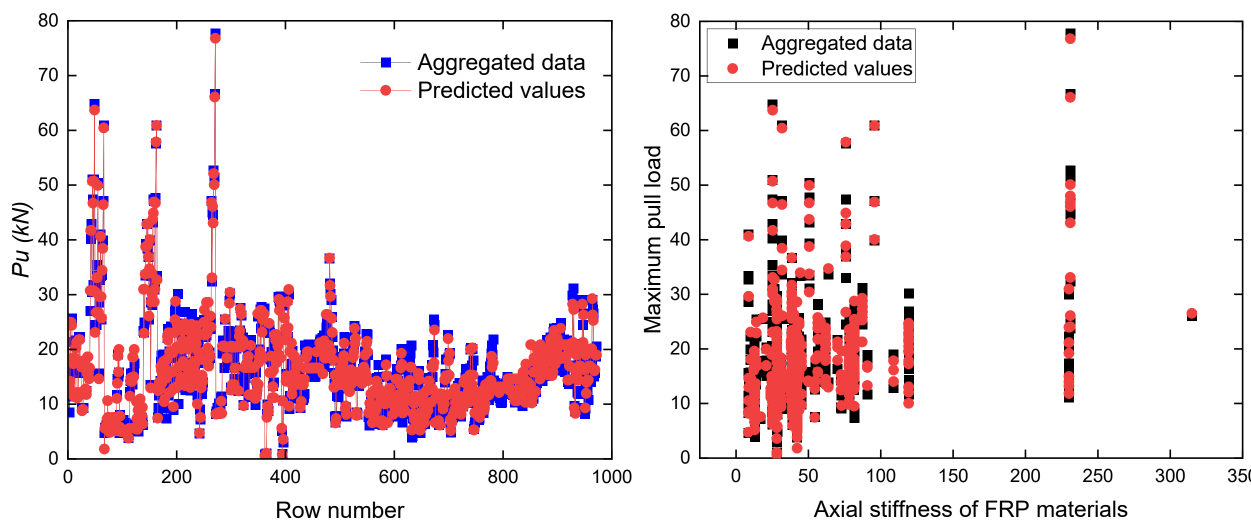

(a) Predicted and aggregated values (b) Maximum pull load against axial stiffness

Fig. 7. Performance of the developed model

The sensitivity analysis establishing the strength of each input parameter in the proposed models is conducted using the Cosine Amplitude method (CAM). This method has been used by various researchers [31,38] and has been adjudged suitable for the evaluation of model sensitivity due to its robustness in understanding how multiple parameters simultaneously affect a system. [88]. The proposed CAM equation is presented in Eq. (21).

$$IIF = \frac{\sum_{i=1}^{n}\left(M_i^{in} \times M_i^{out}\right)}{\sqrt{\sum_{i=1}^{n}\left(M_i^{in}\right)^2 \sum_{i=1}^{n}\left(M_i^{out}\right)^2}} \tag{5}$$

where IIF is the influence of the inputs, M_i^{in} and M_i^{out} are the model inputs and output, respectively. The importance of the input parameters based on the sensitivity analysis is presented in Fig. 8.

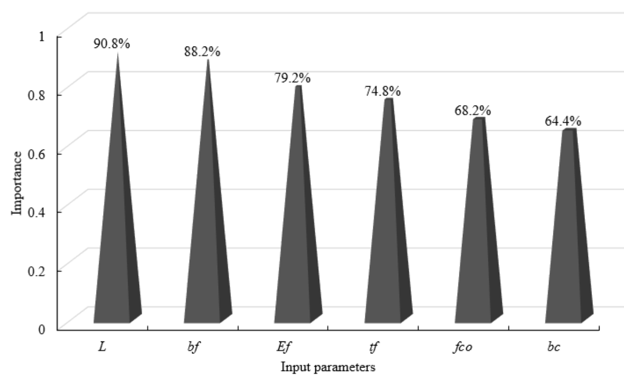

Fig. 8. Importance of the input parameters on the developed model

The order of influence of the model parameters on the predicted P_u is $L > b_f > E_f > t_f > f_{co} > b_c$.

5. Conclusion

This paper presents a gene expression programming model trained on existing data on the maximum bond strength of externally bonded FRP-to-concrete. A test database of 983 datasets was aggregated from the existing studies. The datasets comprise a wide range of strength of concrete, bond length, width of FRP sheet, width of concrete block, axial stiffness of FRP sheet, and maximum pull load. The strength of the concrete, bond length, width of FRP sheet, width of concrete block, and axial stiffness of FRP sheet, are the input parameters used to predict the maximum bond strength. The results of the current study show the potential of utilizing modern computing techniques in predicting the maximum bond strength and identifying the importance of input parameters that affect the maximum bond strength of FRP-to-concrete. The following significant conclusions could also be drawn from the results of this study:

- The slope of the regression lines for the testing and training data is above 90%, which resulted in a correlation between the predicted values and the aggregated data, as well as a small integral absolute error.
- The performance of the developed mathematical-based expression shows an undeniably small disparity compared to the aggregated data and different axial stiffness of the FRP materials.
- Based on the sensitivity analysis, all the input parameters have an importance of greater than 60%. The bond length and width significantly affect the maximum bond strength of FRP-to-concrete. Then followed by the elastic modulus and the thickness of the FRP materials.

  Include any limitation to inform recommendation for further study.

Conflict of Interest

The author declares no conflict of interest.

References

The authors would like to thank the Editor and Reviewers for their beneficial recommendations that helped shape this study.

References

[1]. Dalgic K.D., Ispir M., and Ilki A. Cyclic and monotonic compression behavior of CFRP-jacketed damaged noncircular concrete prisms. J Compos Constr. 2016, 20(1):04015040.

[2]. Ma G., Li H., and Wang J. Experimental Study of the Seismic Behavior of an Earthquake-Damaged Reinforced Concrete Frame Structure Retrofitted with Basalt Fiber-Reinforced Polymer. J Compos Constr. 2013, 17(6):04013002.

[3]. Lim J.C., and Ozbakkaloglu T. Lateral strain-to-axial strain relationship of confined concrete. J Struct Eng. 2015, 141(5):04014141.

[4]. Wu Y.F., and Wei Y.Y. General stress-strain model for steel-and FRP-confined concrete. J Compos Constr. 2015, 19(4):04014069.

[5]. Tsonos A.G. Effectiveness of CFRP-jackets and RC-jackets in post-earthquake and pre-earthquake retrofitting of beam–column subassemblages. Eng Struct. 2008, 30(3):777–93.

[6]. Tijani I.A., Jiang C., Lim C.W., and Wu Y.F. Effect of Load Eccentricity on the Mechanical Response of FRP-Confined Predamaged Concrete under Compression. J Compos Constr. 2020, 24(5):04020057.

[7]. Tijani I.A., Wu Y.F., and Lim C.W. Effects of pre-damage on stress-strain relationship of partially confined concrete. ACI Struct J. 2020, 118(1):61–72.

[8]. Tijani I.A., Jiang C., Lim C.W., and Wu Y.-F. Eccentrically Loaded Concrete under Nonuniform Passive Confinement. J Struct Eng. 2022, 148(1).

[9]. Chen J.F., and Teng J.G. Anchorage Strength Models for FRP and Steel Plates Bonded to Concrete. J Struct Eng. 2001, 127(7):784–91.

[10]. Monaldo E., Nerilli F., and Vairo G. Effectiveness of some technical standards for debonding analysis in FRP-concrete systems. Compos Part B Eng. 2019, 160:254–67.

[11]. Savoia M., Ferracuti B., and Mazzotti C. Non linear bond-slip law for FRP-concrete interface. In: Fibre-Reinforced Polymer Reinforcement for Concrete Structures. World Scientific Publishing Company; 2003. p. 163–72.

[12]. Dai J., Ueda T., and Sato Y. Development of the Nonlinear Bond Stress–Slip Model of Fiber Reinforced Plastics Sheet–Concrete Interfaces with a Simple Method. J Compos Constr. 2005, 9(1):52–62.

[13]. Wu Z., Islam S.M., and Said H. A Three-Parameter Bond Strength Model for FRP—Concrete Interface. J Reinf Plast Compos. 2009, 28(19):2309–23.

[14]. Wu Y.F., and He L. Width effect of interfacial bond characteristics. Constr Build Mater. 2019, 220:712–26.

[15]. FIB. Externally bonded FRP reinforcement for RC structures. International Federation for Structural Concrete (fib). 2001.

[16]. Arya C., Clarke J.L., Kay E.A., and O'Regan P.D. TR 55: Design guidance for stengthening concrete structures using fibre composite materials: a review. Eng Struct. 2002, 24(7):889–900.

[17]. Serbescu A., Guadagnini M., and Pilakoutas K. Standardised double-shear test for

determining bond of FRP to concrete and corresponding model development. Compos Part B Eng. 2013, .

[18]. Dai J.G., and Ueda T. Local bond stress slip relations for FRP sheets-concrete interfaces. In: Fibre-Reinforced Polymer Reinforcement for Concrete Structures. World Scientific Publishing Company; 2003. p. 143–52.

[19]. Lu X.Z., Teng J.G., Ye L.P., and Jiang J.J. Bond-slip models for FRP sheets/plates bonded to concrete. Eng Struct. 2005, 27(6):920–37.

[20]. Wu Y.F., and Jiang C. Quantification of bond-slip relationship for externally bonded FRP-to-concrete joints. J Compos Constr. 2013, 17(5):673–86.

[21]. Pan J.L., and Wu Y.F. Analytical modeling of bond behavior between FRP plate and concrete. Compos Part B Eng. 2014, 61:17–25.

[22]. Van Gemert D. Force transfer in epoxy bonded steel/concrete joints. Int J Adhes Adhes. 1980, 1(2):67–72.

[23]. Yoshizawa H., and Wu Z. Analysis of debonding fracture properties of CFS strengthened member subject to tension. Proceedings of 3rd international symposium on non-metallic (FRP) reinforcement for concrete structures. 1997.

[24]. Khalifa A., Gold W.J., Nanni A., and Abdel Aziz M.I. Contribution of externally bonded FRP to shear capacity of RC flexural members. J Compos Constr. 1998, .

[25]. Chaallal O., Nollet M.J., and Perraton D. Strengthening of reinforced concrete beams with externally bonded fiber-reinforced-plastic plates: design guidelines for shear and flexure. Can J Civ Eng. 1998, 25(4):692–704.

[26]. Naser M.Z. Machine learning assessment of fiber-reinforced polymer-strengthened and reinforced concrete members. ACI Struct J. 2020, 117(6).

[27]. Perera R., Barchín M., Arteaga A., and Diego A. De. Prediction of the ultimate strength of reinforced concrete beams FRP-strengthened in shear using neural networks. Compos Part B Eng. 2010, 41(4).

[28]. Tanarslan H.M., Kumanlioglu A., and Sakar G. An anticipated shear design method for

reinforced concrete beams strengthened with anchoraged carbon fiber-reinforced polymer by using neural network. Struct Des Tall Spec Build. 2015, 24(1).

[29]. Fathollahi-Fard A.M., Ahmadi A., Goodarzian F., and Cheikhrouhou N. A bi-objective home healthcare routing and scheduling problem considering patients' satisfaction in a fuzzy environment. Appl Soft Comput. 2020, 93:106385.

[30]. Naderpour H., and Mirrashid M. Estimating the compressive strength of eco-friendly concrete incorporating recycled coarse aggregate using neuro-fuzzy approach. J Clean Prod. 2020, 265:121886.

[31]. Lawal A.I., Kwon S., Hammed O.S., and Idris M.A. Blast-induced ground vibration prediction in granite quarries: An application of gene expression programming, ANFIS, and sine cosine algorithm optimized ANN. Int J Min Sci Technol. 2021, 31(2):265–77.

[32]. Lawal A.I., and Idris M.A. An artificial neural network-based mathematical model for the prediction of blast-induced ground vibrations. Int J Environ Stud. 2020, 77(2):318–34.

[33]. Shahmansouri A.A., Yazdani M., Ghanbari S., Akbarzadeh Bengar H., Jafari A., and Farrokh Ghatte H. Artificial neural network model to predict the compressive strength of eco-friendly geopolymer concrete incorporating silica fume and natural zeolite. J Clean Prod. 2021, 279:123697.

[34]. Emamian S.A., and Eskandari-Naddaf H. Effect of porosity on predicting compressive and flexural strength of cement mortar containing micro and nano-silica by ANN and GEP. Constr Build Mater. 2019, 218:8–27.

[35]. Mahdinia S., Eskandari-Naddaf H., and Shadnia R. Effect of cement strength class on the prediction of compressive strength of cement mortar using GEP method. Constr Build Mater. 2019, 198:27–41.

[36]. Sadowski Ł., Piechówka-Mielnik M., Widziszowski T., Gardynik A., and Mackiewicz S. Hybrid ultrasonic-neural prediction of the compressive strength of environmentally friendly concrete screeds with high volume of waste quartz mineral dust. J Clean Prod. 2019, 212:727–40.

[37]. Ashrafian A., Taheri Amiri M.J., Rezaie-Balf M., Ozbakkaloglu T., and Lotfi-Omran O.

Prediction of compressive strength and ultrasonic pulse velocity of fiber reinforced concrete incorporating nano silica using heuristic regression methods. Constr Build Mater. 2018, 190:479–94.

[38]. Lawal A.I., Aladejare A.E., Onifade M., Bada S., and Idris M.A. Predictions of elemental composition of coal and biomass from their proximate analyses using ANFIS, ANN and MLR. Int J Coal Sci Technol. 2021, 8(1):124–40.

[39]. Lawal A.I., and Kwon S. Application of artificial intelligence in rock mechanics: An overview. J Rock Mech Geotech Eng. 2021, (1):248–66.

[40]. Said K.O., Onifade M., Lawal A.I., and Githiria J.M. An Artificial Intelligence-based Model for the Prediction of Spontaneous Combustion Liability of Coal Based on Its Proximate Analysis. Combust Sci Technol. 2020, :1–18.

[41]. T.S. Tanaka. Resisting Mechanism of Reinforced Concrete Beams with CFS as Shear Reinforcement. Hokkaido University, Hokkaido, Japan; 1996.

[42]. Naser M.Z. Heuristic machine cognition to predict fire-induced spalling and fire resistance of concrete structures. Autom Constr. 2019, 106:102916.

[43]. Algaifi H.A., Alqarni A.S., Alyousef R., Bakar S.A., Ibrahim M.H.W., Shahidan S., et al. Mathematical prediction of the compressive strength of bacterial concrete using gene expression programming. Ain Shams Eng J. 2021, .

[44]. Tijani I.A., Lawal A.I., and Kwon S. Machine learning techniques for prediction of ultimate strain of FRP-confined concrete. Struct Eng Mech An Int ' l J. 2022, 84(1):101–11.

[45]. Alabi S.A., Arum C., Adewuyi A.P., Arum R.C., Afolayan J.O., and Mahachi J. Mathematical model for prediction of compressive strength of ternary blended cement concrete utilizing gene expression programming. Sci African. 2023, 22.

[46]. Tijani I.A., Lawal A.I., Ogunsola N.O., and Kwon S. Prediction of ultimate strength of FRP-confined predamaged concrete using backward multiple regression motivated soft computing methods. Sci Iran. 2023, 0(0).

[47]. Fares A., Tijani I.A., Rui Z., and Zayed T. Leak detection in real water distribution networks

based on acoustic emission and machine learning. Environ Technol. 2022, :1–17.

[48]. Tijani I.A., Abdelmageed S., Fares A., Fan K.H., Hu Z.Y., and Zayed T. Improving the leak detection efficiency in water distribution networks using noise loggers. Sci Total Environ. 2022, 821:153530.

[49]. Liu R., Tariq S., Tijani I.A., Fares A., Bakhtawar B., Fan H., et al. Data-Driven Approaches for Vibroacoustic Localization of Leaks in Water Distribution Networks. Environ Process. 2024, 11(1).

[50]. Ferreira C. Gene expression programming: A new adaptive algorithm for solving problems. Complex Syst. 2011, 13(2):87–129.

[51]. Tijani I.A., and Zayed T. Gene expression programming based mathematical modeling for leak detection of water distribution networks. Measurement. 2022, 188:110611.

[52]. Shi J., Zhu H., Wu Z., Seracino R., and Wu G. Bond Behavior between Basalt Fiber–Reinforced Polymer Sheet and Concrete Substrate under the Coupled Effects of Freeze-Thaw Cycling and Sustained Load. J Compos Constr. 2013, 17(4):530–42.

[53]. Wu Y.F., and Liu K. Characterization of Mechanically Enhanced FRP Bonding System. J Compos Constr. 2013, 17(1):34–49.

[54]. Zhou Y., Fan Z., Du J., Sui L., and Xing F. Bond behavior of FRP-to-concrete interface under sulfate attack: An experimental study and modeling of bond degradation. Constr Build Mater. 2015, 85:9–21.

[55]. Al-Allaf M.H., Weekes L., Augusthus-Nelson L., and Leach P. An experimental investigation into the bond-slip behaviour between CFRP composite and lightweight concrete. Constr Build Mater. 2016, 113:15–27.

[56]. Irshidat M.R., and Al-Saleh M.H. Effect of using carbon nanotube modified epoxy on bond-slip behavior between concrete and FRP sheets. Constr Build Mater. 2016, 105:511–8.

[57]. Shrestha J., Zhang D., and Ueda T. Bond-Slip Models for FPR-Concrete Interfaces Subjected to Moisture Conditions. Int J Polym Sci. 2017, 2017.

[58]. Mostofinejad D., Heydari Mofrad M., Hosseini A., and Heydari Mofrad H. Investigating

the effects of concrete compressive strength, CFRP thickness and groove depth on CFRP-concrete bond strength of EBROG joints. Constr Build Mater. 2018, 189:323–37.

[59]. Sui L., Luo M., Yu K., Xing F., Li P., Zhou Y., et al. Effect of engineered cementitious composite on the bond behavior between fiber-reinforced polymer and concrete. Compos Struct. 2018, 184:775–88.

[60]. Wan B., Jiang C., and Wu Y.F. Effect of defects in externally bonded FRP reinforced concrete. Constr Build Mater. 2018, 172:63–76.

[61]. Yuan C., Chen W., Pham T.M., and Hao H. Bond behavior between basalt fibres reinforced polymer sheets and steel fibres reinforced concrete. Eng Struct. 2018, 176:812–24.

[62]. Bizindavyi L., and Neale K.W. Transfer lengths and bond strengths for composites bonded to concrete. J Compos Constr. 1999, .

[63]. Gao L., Zhang F., Liu J., Lu X., and Gao H. Experimental and numerical study on the interfacial bonding characteristics of FRP-to-concrete joints with mechanical fastening. Constr Build Mater. 2019, 199:456–70.

[64]. Moghaddas A., Mostofinejad D., and Ilia E. Empirical FRP-concrete effective bond length model for externally bonded reinforcement on the grooves. Compos Part B Eng. 2019, 172.

[65]. Moghaddas A., and Mostofinejad D. Empirical FRP-Concrete Bond Strength Model for Externally Bonded Reinforcement on Grooves. J Compos Constr. 2019, 23(2):04018080.

[66]. Moshiri N., Tajmir-Riahi A., Mostofinejad D., Czaderski C., and Motavalli M. Experimental and analytical study on CFRP strips-to-concrete bonded joints using EBROG method. Compos Part B Eng. 2019, 158:437–47.

[67]. Mostofinejad D., Sanginabadi K., and Eftekhar M.R. Effects of coarse aggregate volume on CFRP-concrete bond strength and behavior. Constr Build Mater. 2019, 198:42–57.

[68]. Wei M.W., Xie J.H., Zhang H., and Li J.L. Bond-slip behaviors of BFRP-to-concrete interfaces exposed to wet/dry cycles in chloride environment. Compos Struct. 2019, 219:185–93.

[69]. Yuan C., Chen W., Pham T.M., Hao H., Jian C., and Shi Y. Strain rate effect on interfacial

bond behaviour between BFRP sheets and steel fibre reinforced concrete. Compos Part B Eng. 2019, 174:107032.

[70]. Li Z.X., Zhang X.., and Shi Y.. Experimental study on the dynamic bond behavior between CFRP and concrete under different slip rates. Eng Struct. 2020, 216.

[71]. Wang Y.L., Guo X.Y., Shu S.Y.H., Guo Y.C., and Qin X.M. Effect of salt solution wet-dry cycling on the bond behavior of FRP-concrete interface. Constr Build Mater. 2020, 254:119317.

[72]. Nakaba K., Kanakubo T., Furuta T., and Yoshizawa H. Bond Behavior between Fiber-Reinforced Polymer Laminates and Concrete. ACI Struct J. 2001, 98(3):1–9.

[73]. Dai J., Sato Y., and Ueda T. Improving the load transfer and effective bond length for FRP composites bonded to concrete. In: Proceedings of the Japan Concrete Institute. 2002. p. 1423–8.

[74]. Yao J., Teng J.G., and Chen J.F. Experimental study on FRP-to-concrete bonded joints. Compos Part B Eng. 2005, 36(2):99–113.

[75]. Toutanji H.A., Saxena P., Zhao L., and Ooi T. Prediction of Interfacial Bond Failure of FRP–Concrete Surface. J Compos Constr. 2007, 11(4):427–36.

[76]. Ko H., and Sato Y. Bond Stress–Slip Relationship between FRP Sheet and Concrete under Cyclic Load. J Compos Constr. 2007, 11(4):419–26.

[77]. Hosseini A., and Mostofinejad D. Effect of groove characteristics on CFRP-to-concrete bond behavior of EBROG joints: Experimental study using particle image velocimetry (PIV). Constr Build Mater. 2013, 49:364–73.

[78]. Bilotta A., Ludovico M. Di, and Nigro E. FRP-to-concrete interface debonding: Experimental calibration of a capacity model. Compos Part B Eng. 2011, 42(6):1539–53.

[79]. Tijani I.A., Wu Y.F., and Lim C.W. Energy balance method for modeling ultimate strain of fiber-reinforced polymer-repaired concrete. Struct Concr. 2020, 21(2):804–20.

[80]. Cao Y.G., Wu Y.F., and Li X.Q. Unified model for evaluating ultimate strain of FRP confined concrete based on energy method. Constr Build Mater. 2016, 103,:23–35.

[81]. Arıoglu N., Girgin Z.C., and Arıoglu E. Evaluation of ratio between splitting tensile strength and compressive strength for concretes up to 120 MPa and its application in strength criterion. ACI Mater J. 2006, 103(1):18–24.

[82]. Ferreira C. Gene expression programming: Mathematical modeling by an artificial intelligence. In: Studies in Computational Intelligence. 2nd ed. Springer; 2006. p. 478.

[83]. Lawal A.I., Olajuyi S.I., Kwon S., and Onifade M. A comparative application of the Buckingham π (pi) theorem, white-box ANN, gene expression programming, and multilinear regression approaches for blast-induced ground vibration prediction. Arab J Geosci. 2021, 14(12):1073.

[84]. Teodorescu L., and Sherwood D. High energy physics event selection with gene expression programming. Comput Phys Commun. 2008, 178(6):409–19.

[85]. Iqbal M., Zhao Q., Zhang D., Jalal F.E., and Jamal A. Evaluation of tensile strength degradation of GFRP rebars in harsh alkaline conditions using non-linear genetic-based models. Mater Struct. 2021, 54(5):190.

[86]. Wu Y.F., and Cao Y.G. Energy balance method for modeling ultimate strain of confined concrete. ACI Struct J. 2017, 114(2):373–81.

[87]. Girgin Z.C., Arioglu N., and Arioglu E. Evaluation of strength criteria for very-high-strength concretes under triaxial compression. ACI Struct J. 2007, 104(3):278–84.

[88]. Jong Y.H., and Lee C.I. Influence of geological conditions on the powder factor for tunnel blasting. Int J Rock Mech Min Sci. 2004, 41:533–8.